

ENERGY RECOVERY LINACS FOR LIGHT SOURCES

RYOICHI HAJIMA

*Quantum Beam Science Directorate, Japan Atomic Energy Agency
Tokai, Ibaraki 319-1195, Japan*

Energy-recovery linac (ERL), which can generate an electron beam having a high-average current and a small-emittance with the complete manipulation of electron beams in the transverse and longitudinal phase space, is expected to realize future light sources for various photon energies from terahertz to X and γ -rays. In this paper, we present an overview of the history, current status, and future prospects of ERLs for light sources. Research activities on the critical components of the ERLs, such as electron guns and superconducting cavities, are also described.

Keywords: ERL; energy-recovery linac; FEL; free-electron laser; superconducting linac.

1. Introduction

Energy-recovery linac (ERL) is a new class of electron accelerators used for generating an electron beam of high-average current and small emittance. In an energy-recovery linac, an electron beam from an injector is accelerated by a time-varying rf field stored in a superconducting linear accelerator; the beam is transported to a recirculation loop. In the recirculation loop, the beam is utilized for particular applications such as X-ray generation. After the recirculation, the spent electron beam is injected again into the superconducting accelerator so that the electrons are decelerated. This deceleration can be accomplished by putting the electrons in the phase opposite to the acceleration, as shown in Fig. 1. Therefore, the energy of the accelerated electrons is converted back into the rf energy and recycled to accelerate the succeeding electrons.

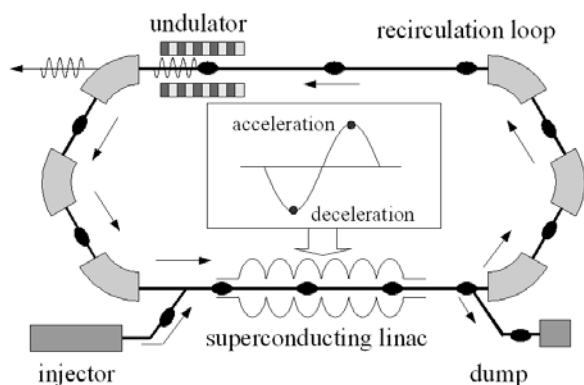


Figure 1. Principle of energy-recovery linac. The electron beam is accelerated in the superconducting linac and utilized for the photon

generation. The spent beam is decelerated in the same linac to recycle the beam energy.

The energy recovery technology has a significant impact on modern accelerator applications because the ERL can accelerate a high-power electron beam with small-capacity rf generators. In addition to this excellent conversion efficiency from the electric power to the electron beam power, the ERL has an advantage essential to the generation of high-brightness electron beams. Since an electron bunch in an ERL goes to a beam dump after deceleration and another fresh electron bunch is accelerated at every turn, the electron beam in the ERL maintains a small emittance. Moreover, we can make the manipulation of the electron beam in the transverse and the longitudinal directions flexible in order to produce a tightly focused beam or a short electron bunch of femtoseconds. The beam brightness of an ERL can be increased by adopting a high-brightness injector such as a photocathode electron gun, whose performance has been improved significantly in the recent years. Therefore, the ERL is considerably different from a storage ring in which the emittance and the temporal duration of electron bunches are determined by the equivalent state of the electron beam dynamics after bunch thermalization during a number of turns.

The ERL is currently considered an important platform of future light sources and as a driver of nuclear physics applications. There are many ERL projects towards these applications and extensive research and development of critical components for these ERLs is in progress; this research covers electron

guns for obtaining a high-average current and a small emittance, superconducting cavities for accelerating a high-average current, and beam dynamics specific to the ERLs.

In the present paper, we present an overview of the history, current status, and future prospects of ERLs. Research activities on the critical components of the ERL, such as electron guns and superconducting cavities, are also described. We should note that ERLs play an important role in future nuclear physics applications such as electron cooling in an ion collider and electron-ion colliders [1]. In the present review, however, we focus on the ERLs for light source applications.

2. Invention of ERL and Early Experiments

In this section, we discuss the early history of ERL from the first proposal of ERL in 1965 to the experiments in the 1980s.

2.1. First Proposal of the ERL for High-Energy Colliders

The idea of an energy recovery linac was first proposed in 1965 by M. Tigner as a variant of a high-energy electron collider [2]. Figure 2 is an electron collider with the energy-recovery technique presented in the abovementioned paper. In this electron collider, two rf linear accelerators generate two high-energy electron beams to collide with each other at the interaction point in experiments called the clashing-beam experiments. Each electron beam after the interaction is injected into the opposite accelerating structure for deceleration. The beams lose their energy during the deceleration, and the energy is converted back into rf energy to accelerate the succeeding electron beams.

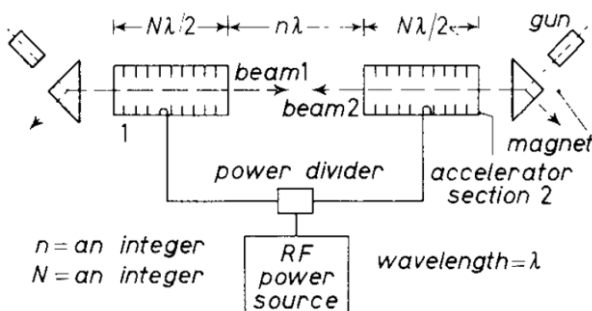


Figure 2. Electron collider using energy-recovery technique proposed by M. Tigner in 1965 [2].

It was claimed that a combination of a superconducting accelerating structure and the energy-recovery technique enables one to generate high-energy high-current electron beams with a practical-sized rf generator. As a result, such a collider achieves a luminosity comparable to or even higher than that of a collider utilizing a storage ring.

In the energy-recovery linac collider shown in Fig. 1, the two beam currents must be kept equal very precisely in order for maintaining the energy recovery. In order to solve this difficulty, another layout of the energy-recovery collider was presented, as depicted in Fig. 3, where an electron beam from a linac is reflected by a 180° arc to collide with itself and re-enter the same linac for the energy recovery.

In the last paragraph of Tigner's paper, there is a sentence: *The energy recovery technique might also be useful in experiments other than clashing beam type.* This prediction became a reality 40 years from then.

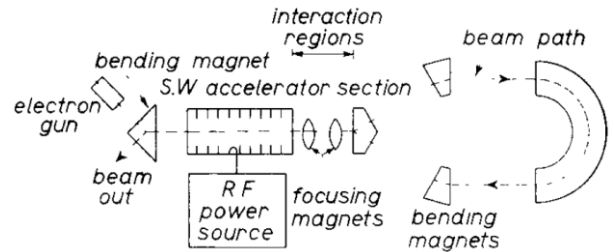


Figure 3. Single-beam electron collider with energy-recovery technique [2].

2.2. ERL Experiments in the early years

The first accelerator that exhibited energy recovery was the Chalk River Reflexotron, which was a double-pass linac consisting of an S-band normal conducting standing wave structure and a reflecting magnet similar to the apparatus shown in Fig. 3. In the Reflexotron, the electron beam passed through the S-band accelerating structure twice achieving second pass energies of 5 to 25 MeV depending on the position of the reflecting magnet relative to the accelerating structure [3]. The energy variability down to 5 MeV was obviously achieved by deceleration of the electron beam in the second pass, which was energy recovery, although there was no statement of the term "energy recovery" in the paper.

The invention of a free-electron laser (FEL) by J. Madaay [4] and successful demonstration of the first FEL at Stanford University [5, 6] opened a new era of

electron accelerator application: the use of an electron accelerator as a source of energy-tunable coherent photon beams.

In the development of an FEL, improvement of the total efficiency from the wall-plug electricity to the FEL power became a matter of concern, especially for high power availability. The conversion efficiency from an electron beam to an optical beam in an FEL is limited by the bandwidth of FEL small-signal gain curve, which is proportional to the derivative of the spontaneous emission spectrum [5]. Thus, the FEL conversion efficiency, η , is given as a function of the number of undulator periods N_u , $\eta \sim 1/(4N_u)$, which is usually around a few percent. Therefore, recycling the spent electron beam is the key to improve the total efficiency of the FEL.

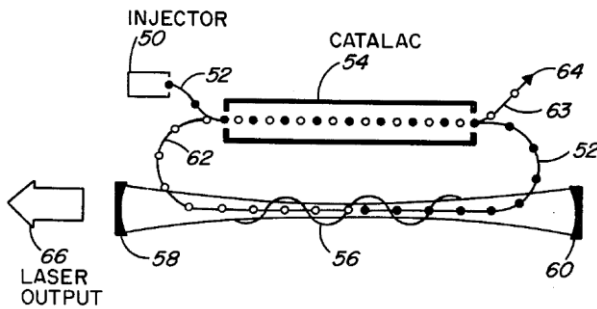


Figure 4. Apparatus of high-efficiency FEL with energy recovery in a US Patent. The apparatus was named Catalac [7].

C. Brau *et al.* at Los Alamos National Laboratory (LANL) applied for a patent for an apparatus of high-efficiency FEL with the energy-recovery technique [7]. The apparatus is completely the same as that of the ERL-FELs in operation today and consists of an injector, an rf linac, an undulator, and a recirculation loop, as shown in Fig. 4. In the patent, they named the rf accelerator/decelerator energy recovery device Catalac (catalytic linac) because Catalac acts as a catalyst to provide an electron beam to the FEL system without suffering from net beam loading. The patent was applied for in 1979 and issued in 1982.

An FEL utilizing an energy-recovery electrostatic accelerator was developed at University of California Santa Barbara (UCSB) in 1984 [8, 9]. The FEL was operated at a sub-millimeter wavelength by using a 3-MV electrostatic accelerator, Pelletron. As shown in Fig. 5, the electron beam after the FEL lasing is transported back to the high-voltage terminal for beam recovery, where the electron beam is decelerated and

sent to a beam collector at the high-voltage terminal of the Pelletron. Therefore, the recirculation works as electron charge recovery as well as energy recovery. This recirculation permits operation at an average current of 1.25 A for a 50 μ s macropulse despite that the fact the charging current of the Pelletron is considerably smaller than the beam current. The UCSB FEL does not use an rf linac but is a type of energy-recovery accelerator in the broad sense of the term.

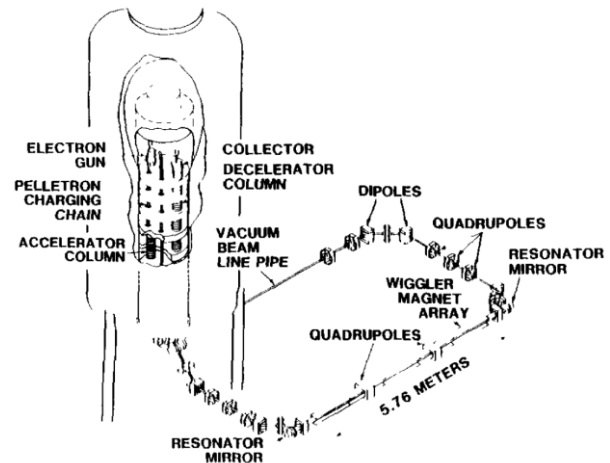


Figure 5. Energy-recovery electrostatic accelerator for sub-millimeter FEL at University of California, Santa Barbara [9].

The research group at LANL constructed an energy-recovery linac for a high-power FEL in 1986 [10]. The ERL utilized a particular type of rf structure, where two rf linacs, one for acceleration and the other for deceleration, are connected by a resonant bridge coupler, as shown in Fig. 6. The accelerator consists of two 10-MeV normal-conducting standing-wave structures operated at 1300 MHz in order to obtain a 20-MeV electron beam for FEL lasing. Each decelerator is electrically the mirror image of its corresponding accelerator. The linac was operated in a pulsed mode with a duration of 100-120 μ s. In the experiment, the electron beam was decelerated to \sim 3.5 MeV in the lowest case. The energy-recovery system was operated during FEL lasing at an extraction efficiency of 0.7%, an average current of 0.1 A, and an deceleration current of 68%. The ERL suffered from beam instabilities, which were caused by a time-varying beam loss at the 60° bends after the accelerator. The 60° bends were designed to scrape a low-energy tail of the electron beam, \sim 25% of the beam current. A fluctuation of the beam energy at the accelerator exit caused a change in

the fraction scraped and in the charge reaching the decelerators, changing the amount of energy recovered.

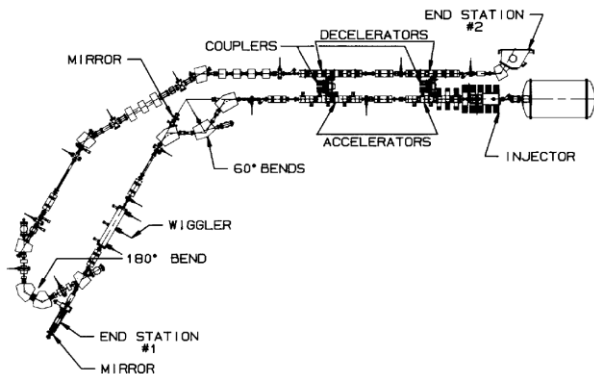


Figure 6. Energy-recovery linac FEL developed at Los Alamos National Laboratory. Two L-band normal conducting linacs for acceleration and deceleration are connected by a resonant bridge coupler [10].

A same-cell energy-recovery experiment was carried out at the superconducting FEL of Stanford University in 1986 [11]. Figure 7 shows a schematic representation of the superconducting linac consisting of a 5-MeV injector, a 50-MeV linac, and a recirculation system. The recirculation system was primarily developed for energy doubling, in which the electron beam was accelerated twice in the linac in order to operate the FEL at a shorter wavelength with this high-energy electron beam. The recirculation system, however, had a path-length controllability to operate the linac in the energy-recovery mode. Figure 8 shows the net rf power required by one of the accelerating cavities in the energy-recovery mode, where the vertical axis is the power incident upon the cavity minus the power reflected. The two traces in the figure correspond to two conditions: with and without a recirculated beam. As we see in the figure, the beam loading in the cavity was compensated for by two beams: acceleration and deceleration. The recirculation system was installed upstream of the FEL, and the energy-recovery operation was demonstrated without FEL lasing.

The experiments at LANL and Stanford University demonstrated the energy-recovery operation in limited ways. The LANL experiment revealed that beam instability should be taken into consideration in the design and operation of ERLs. These experiments, however, encouraged research activities of high-power FELs utilizing an energy-recovery linac, which resulted in the construction of high-power FEL facilities at JLAB, JAEA, and BINP. We see these FEL facilities in the later section.

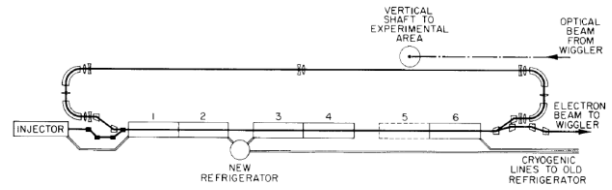


Figure 7. Recirculating superconducting linac for FEL at Stanford University. An energy-recovery experiment was conducted in 1986 [11].

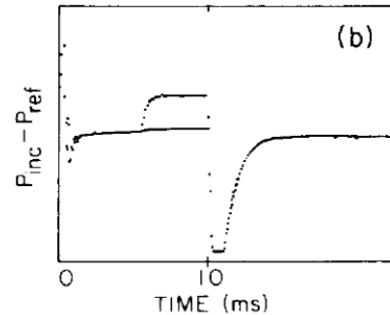


Figure 8. Evidence of the energy-recovery operation at the Stanford superconducting linac. Net rf power during a macropulse of 10 ms is plotted for two cases: with recirculation and without recirculation. The electron beam loading, from 5 ms to 10 ms, is compensated for by the energy-recovery with a recirculating beam [11].

3. Energy-Recovery Linacs Operated Thus Far and In Operation

3.1. High-Power FELs at Jefferson Laboratory

The energy-recovery linac at Thomas Jefferson National Accelerator Facility (JLAB) was the first facility dedicated to a high-power FEL with same-cell energy recovery. The JLAB-FEL program was initiated in 1995 on the basis of the idea that at a sufficiently high power there would be economically viable applications of the FEL for industrial activity. After the consideration of the cost model and the availability of the required technology [12, 13], they decided to employ CEBAF cavities to construct IR-demo, a high-power infrared FEL based on the energy-recovery technique.

Figure 9 shows a schematic representation of the IR-demo. The machine can be divided into the following components: an injector, a main linac, a recirculation loop, and an FEL system.

The injector consists of a photocathode DC gun and an injector superconducting linac. The DC gun (350 kV) is equipped with a semiconductor photocathode, GaAs, having a surface of negative electron affinity (NEA). The electron beam extracted from the gun is accelerated

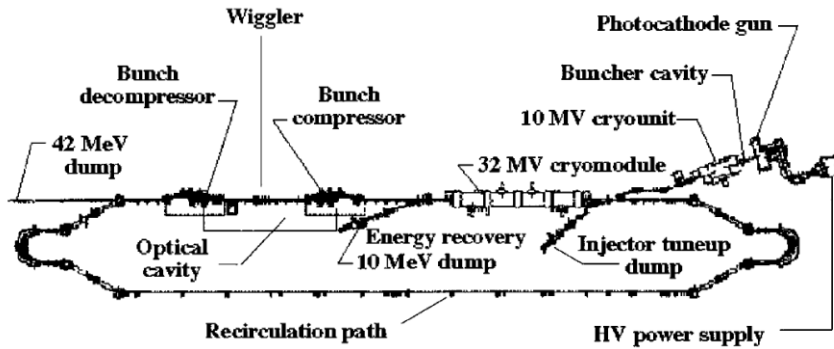


Figure 9. Layout of IR-demo, a high-power FEL based on energy-recovery technique, at Thomas Jefferson National Accelerator Facility [16].

up to 10 MeV by an injector superconducting linac, which contains two CEBAF-type cavities, and injected into the main linac.

The main linac employs a cryomodule developed for CEBAF, which contains four 5-cell cavities operating at 1497 MHz. Each cavity is driven independently by a 5-kW klystron. The cryomodule provides an energy gain of 32 MeV.

The recirculation loop of IR-demo is similar to that of the MIT Bates [14]. Two arcs in the recirculation loop comprise large 180° bends and four small dipoles. This type of arc provides a beam transport of achromatic and isochronous in linear beam dynamics by a combination of a four-dipole chicane and a 180° bend, which have negative and positive R_{56} , respectively. The variable R_{56} is the correlation of the momentum and the path length of an electron. One of the major advantages of the Bates arc for an ERL recirculation loop is the large momentum acceptance, which is particularly important for the operation of a high-power FEL. In the IR-demo, the energy acceptance of the return loop is designed to be 6%. The FEL system was installed before the first arc to take care of the emittance growth due to the coherent synchrotron radiation in the arc.

The electron bunch is compressed to 0.4 ps by a chicane bunch compressor before the FEL undulator. This bunch compression is necessary to obtain a large FEL gain. The bunch is decompressed by another chicane after the FEL lasing and transported to the return arc and reinjected into the main linac for deceleration. The FEL interaction introduces a large energy spread, several percent to 10%, in the electron bunch. This large energy spread causes a serious issue in the energy recovery because the 10% energy spread at 42 MeV results in a 40% energy spread after deceleration to 10 MeV. In order to solve this problem, energy compression is carried out in the return path by

rotating the beam in the longitudinal phase space. In the IR-demo, the momentum compaction of the return path in the first and the second orders, R_{56} and T_{566} , and the deceleration phase are optimized for the best energy compression [15].

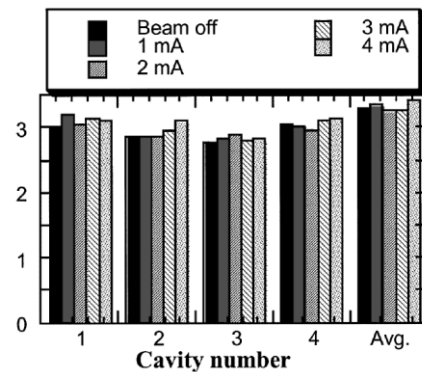


Figure 10. Rf drive power in kilowatts for the first four of the eight cavities and the average of all the eight cavities at the IR-demo. Variation in power is comparable to the fluctuations due to the microphonics [16].

The IR-demo achieved first lasing on June 15, 1998, at a wavelength of $4.9 \mu\text{m}$ without energy recovery. In this case, the beam current was limited to 1.1 mA by the capacity of klystrons for the main linac. After the commissioning of the recirculation loop, the first FEL lasing with the same-cell energy recovery was achieved on March 11, 1999, at a wavelength of $4.9 \mu\text{m}$. In the energy-recovery operation, they could accelerate the beam up to 4.8 mA. The beam current was increased by changing the bunch repetition rate from 18.7 MHz to 74.8 MHz while maintaining the same bunch charge. Figure 10 shows the cryomodule rf power in kilowatts versus the recirculated beam current during the FEL lasing. Perfect energy recovery was confirmed from the fact that the rf drive power was independent of the beam current, as shown in Fig. 10 [16].

In the IR-demo, the FEL power in excess of 2.1 kW was demonstrated, and the FEL lasing at the 2nd, 3rd, and 5th harmonics was also obtained [17].

The experimental proof of the high-power ERL-FEL at the IR-demo was followed by a construction of another ERL-FEL of a higher average power in excess of 10 kW. The 10-kW ERL-FEL was named the IR-upgrade FEL. After the design studies of a driver accelerator [18] and an FEL device [19], the IR-upgrade was completed, as shown in Fig. 11.

The injector has the same configuration as the one used in the IR-demo but is capable of producing an electron beam of 10 mA and 9.2 MeV. The current was doubled by an increase in the single bunch charge from 60 pC to 135 pC while maintaining a repetition rate of 74.8 MHz. The main linac consists of three CEBAF-type cryomodules: the first and the third are conventional 5-cell CEBAF designs, and the central module is based on new 7-cell cavities. The linac is capable of accelerating the injected beam of 9.2 MeV to 160 MeV. The recirculation loop is of the Bates type, same as the IR-demo, but the magnet and vacuum chamber were modified to increase the energy acceptance up to 15%. The FEL wiggler was installed in the long straight section opposite to the main linac.

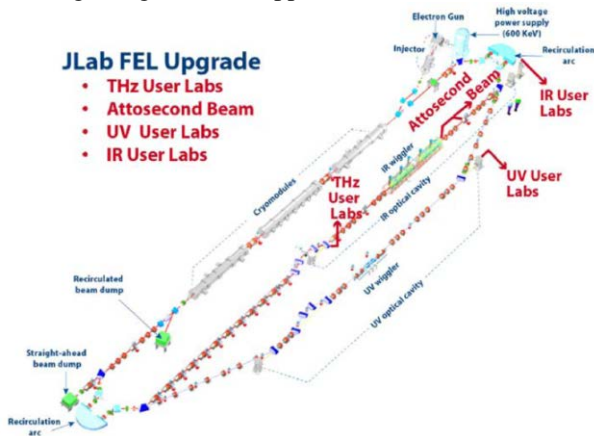


Figure 11. Layout of the IR-upgrade FEL at Jefferson Laboratory [17].

The first lasing of the IR-upgrade FEL was achieved on June 17, 2003, when the beam was operated in a non-ERL mode. FEL lasing with an ERL operation was obtained on August 19, 2003 [20]. Thus far, the FEL power up to 14.2 kW at a wavelength of 1.6 μm was demonstrated. An additional beam line for a UV-FEL is under commissioning [17].

In the IR-upgrade, strong terahertz radiation is also available. This terahertz radiation is generated by a

coherent synchrotron radiation from a short electron bunch passing a dipole magnet just before the FEL wiggler. The radiation from an electron bunch of 400 fs covers 0.1–10 THz with a spectral intensity of a few $10\text{W}/\text{cm}^{-1}$, which is larger by 4–6 orders of magnitude than that of a standard Glycer lamp [21].

A multi-pass beam-break-up phenomenon resulting from the higher-order modes in the superconducting cavities (HOM-BBU) appeared during the commissioning of the IR-upgrade [22]. The issue of HOM-BBU is discussed later in detail.

The experimental demonstration of high-power FELs at JLAB IR-demo and IR-upgrade clearly showed the potential performance of the energy-recovery technique not only for a high-power FEL but also for various types of light source applications of electron accelerators. It was proved that a high-brightness and high-power electron beam generated from ERLs enables one to improve such light-source capability both in spectral brightness and flux.

3.2. High-Power FEL at Japan Atomic Energy Agency

An energy-recovery linac for a high-power FEL was developed at Japan Atomic Energy Agency (JAEA), formerly named Japan Atomic Energy Research Institute (JAERI). The research program of JAEA FEL was initiated in 1987 aiming at the applications of FEL to isotope separation and other basic research of laser and accelerator science for atomic energy [23]. In order to realize a high-power FEL at a wavelength of the infrared region, they decided to utilize a superconducting linac as a driver of the FEL. The FEL was constructed to have a non-ERL configuration; however, they also had an upgrade plan, from the early stage of the project, to modify the FEL into an ERL [24, 25, 26].

The FEL facility was completed in 1994, and the first lasing of FEL was demonstrated in 1998 [27]. The frequency of the superconducting cavity was 499.8 MHz, which was operated in a pulsed mode, the duration of the rf pulse was 3 ms, and the repetition rate was 10 Hz. The electron beam for the FEL was 17 MeV at 5 mA (500 pC, 10.4125 MHz). They improved the injector system in 2000 and attained a shorter bunch duration, a smaller emittance, and smaller time jitters [28]. After the improvement, they could increase the FEL power up to 2.34 kW during a macro pulse in 2001 [29, 30]. This high-power record was attained by high-efficiency

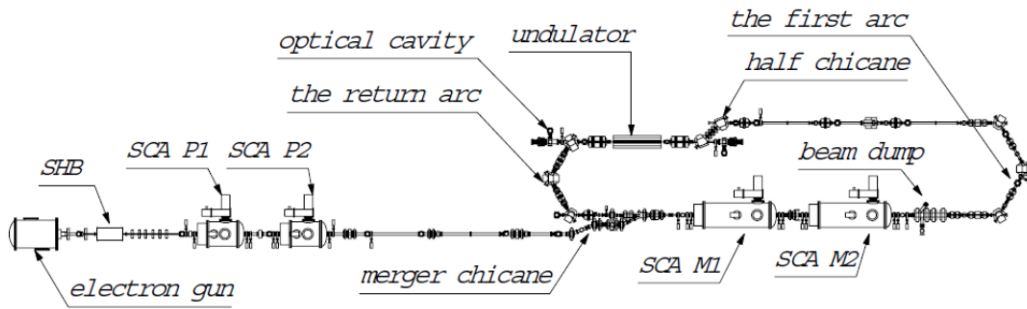


Figure 12. Layout of the 17-MeV energy-recovery linac at Japan Atomic Energy Agency [35].

superradiant lasing as evident by the perfect synchronization of the optical pulse and the electron bunch [31].

After the successful high-power FEL lasing, the machine was reconstructed into an ERL [32]. The original linac was shut down in spring 2001, and the ERL was completed after a half year construction period.

Figure 12 shows a schematic representation of the JAEA ERL FEL. The injector consists of a 230-kV electron gun with a gridded thermionic cathode, an 83.3-MHz subharmonic buncher (SHB), and two cryomodules, each of which contains a single-cell superconducting cavity driven at 499.8 MHz. An electron bunch of 450 pC with a length of 600 ps (FWHM) is generated by a grid pulser at a repetition rate of 20.825 MHz, that is, an average current of 9 mA. The electron bunch is accelerated to 2.5 MeV by two single cells and transported to the merger. The main linac consists of two 5-cell cavities driven at 499.8 MHz. The bunch duration and the normalized emittance at the undulator were 12 ps (FWHM) and 40 mm-mrad (rms), respectively. They employed two 50-kW inductive output tubes (IOTs) for the injector and two 50-kW solid state amplifiers for the main linac.

The design and operation parameters of the superconducting cavities were $E_{acc} = 5$ MV/m, $Q_0 \sim 2 \times 10^9$, $Q_L \sim 2 \times 10^6$, and $(R/Q) = 575 \Omega$ for the 5-cell cavities; $(R/Q) = 115 \Omega$ for the 1-cell cavities; and an operation temperature of 4.5 K. The sum of the static and the dynamic heat loads at 4.5 K for the 5-cell cavity was around 5 W for a duty cycle of 3%. The cavities were contained in stand-alone and zero-boil-off cryostats, which are equivalent to helium containers having cooling refrigerators. Such a cryogenic system has the following advantages: (1) the system is exempted from the regulation of high-pressure gases and (2) the system can be operated for many years without warming up the cryostat.

The recirculation loop consists of two triple-bend arcs and a half chicane before the undulator. Each arc has two families of quadrupoles that enable one to vary R_{56} while maintaining the achromaticity. This variable R_{56} is especially required in the second arc because energy-spread compression is required in the return path. The second arc also has two families of sextupoles to compensate for the second-order aberrations T_{166} , T_{266} , and T_{566} arising from a large energy spread due to the FEL interaction. The energy acceptance of the second arc is 15% to allow high-efficiency FEL lasing [33].

They demonstrated the first energy-recovery operation on February 19, 2002, and the first FEL lasing on August 14, 2002 [34]. The energy recovery was confirmed by the measurement of the rf forward power from the amplifier to the cavity. From the signal shown in Fig. 13, the energy-recovery ratio, which is the ratio of the recovered rf power to the beam power, was evaluated to be 98% by assuming the linearity of the envelope detector. The imperfect energy recovery was attributed to the phase slip of the electrons in the low-energy section of the cavity, 2.5 MeV.

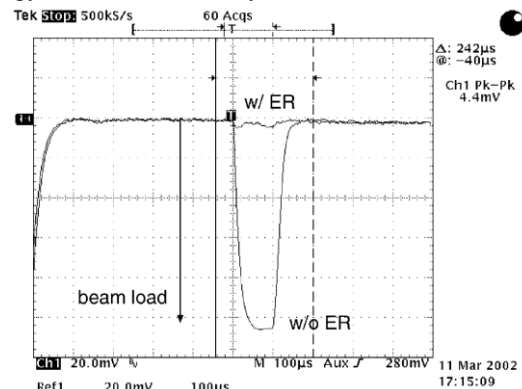


Figure 13. Rf forward power fed into the first superconducting cavity of the main linac at the JAEA ERL. Two waveforms correspond to the case of ERL operation (w/ ER) and non-ERL operation (w/o ER). The beam load is almost canceled during the ERL operation [34].

The FEL lasing with an energy-recovery operation was also successfully achieved. In the lasing, the FEL power and the conversion efficiency were limited by the energy acceptance of the return loop. The maximum FEL power and conversion efficiency were 0.75 kW and 2.5%, respectively [35].

Coherent synchrotron radiation in the millimeter wavelength region was also observed from an electron bunch traveling through the middle dipole magnet in the second arc [36].

3.3. Energy-Recovery Experiment at CEBAF

A GeV-scale energy-recovery experiment was carried out at the Continuous Electron Beam Accelerator Facility (CEBAF) in March 2003 [37]. The CEBAF is a five-pass recirculating superconducting linear accelerator for nuclear physics applications [38,39]. In the energy-recovery experiment, a new beam dump and a $\lambda_{RF}/2$ chicane were installed as shown in Fig. 14. The beam was injected into the linac with energies of 20 MeV or 55 MeV. Each of two linacs was configured to provide 500 MeV of acceleration so that the beam energy after passing two linacs became 1 GeV plus the injection energy. After the acceleration, the beam was transported to a $\lambda_{RF}/2$ chicane to shift the beam to the deceleration phase. Then, the beam was decelerated by two linacs down to an energy that is equal to the injection energy. The beam current was 80 μA for the 55-MeV injection and 1 μA for the 20-MeV injection.

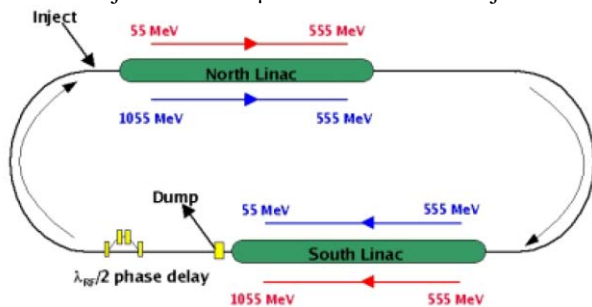


Figure 14. Layout of CEBAF energy-recovery experiment for the 55-MeV injection [37].

This is the energy-recovery experiment of the highest beam energy, 1055 MeV, and the largest peak-to-injection energy ratio, 50:1, thus far.

3.4. High-Power FEL at Budker Institute of Nuclear Physics

In Budker Institute of Nuclear Physics (BINP), they are developing an accelerator-recuperator (or microtron-

recuperator) for a high-power FEL. The first proposal of the accelerator-recuperator was published in 1991, in which a 4-pass racetrack microtron equipped with an FEL undulator at the fourth pass was presented [40]. The concept of the accelerator-recuperator is depicted in Fig. 15, in which an electron beam is accelerated by a multi-pass accelerator, or a racetrack microtron, and utilized for an FEL, and then the beam is decelerated along the same multi-pass orbits in an inverse sequence. Therefore, the accelerator-recuperator is a type of energy-recovery linac. The accelerator-recuperator at BINP aims at a high-power FEL as well as the precedent ERLs at JLAB and JAEA. The accelerator-recuperator, however, has the following distinguishable features: the utilization of a normal-conducting linac and a multi-loop configuration.

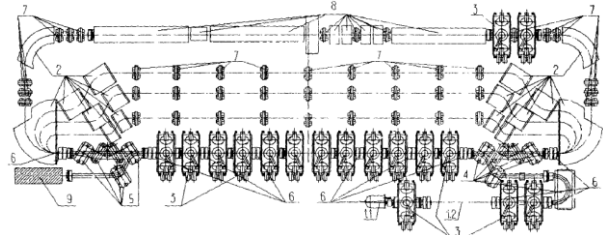


Figure 15. Schematic representation of the accelerator-recuperator proposed at BINP. 1. injector, 11. electron gun, 12. bunching straight section, 2. magnetic system of the 180° bend, 3. rf cavities, 4. magnets of the injection system, 5. magnets of the extraction system, 6. solenoid magnet lenses, 7. quadrupole magnetic lenses, 8. magnetic system of the FEL, 9. beam dump [40].

They are constructing the accelerator-recuperator in two stages. The first stage of the machine has a full-scale rf but only a single orbit. The second stage of the machine is designed to have 4-pass orbits. Figure 16 shows a schematic representation of the first stage of the accelerator-recuperator.

A specific feature of the accelerator-recuperator is the use of the normal conducting cavities for the linac. They employed an array of single-cell cavities driven at 180.4 MHz. A large dimension of the cavity and relatively low accelerating voltage, 700 kV at each cavity, allow one to operate the linac in the CW mode. The cavities are made from bimetal sheets (copper-clad stainless steel sheets with 8 mm of copper and 7 mm of stainless steel), produced by diffusion welding. The cavities are cooled by water during operation. The linac is driven by two groups of rf generators, each of which produces a 600-kW output power. The generator is a four-stage power amplifier, where tetrodes (GU-92A,

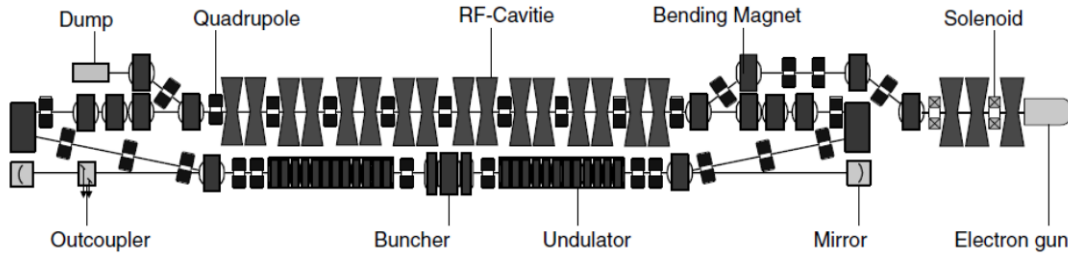


Figure 16. Layout of the first stage of the accelerator-recuperator at the BINP. A normal-conducting linac and an FEL undulator are installed in the vertical plane [42].

GU-101A made by Russian company, SVETLANA) are used for the high-power devices [41].

The injector of the accelerator-recuperator consists of a 300-kV DC electron gun equipped with a gridded thermionic cathode, a buncher cavity, and two accelerating cavities. All the buncher and accelerating cavities are driven at 180.4 MHz, the same frequency as that of the main linac. In the 300-kV DC gun, a train of electron bunches (1500 pC, 1.6 ns, 22.5 MHz) is generated by a home-made pulser. The electron bunch is compressed by the buncher and a drift section and accelerated by the injector cavities. The energy and the temporal duration of the electron bunch at the entrance of the main linac are 1.8 MeV and 100 ps, respectively. The injection merger is a four-dipole chicane with quadrupole magnets. The recirculation loop is installed in the vertical plane.

The first FEL lasing in the accelerator-recuperator was obtained in April 2003 [42]. In the FEL lasing, the electron beam of 12 MeV was transported to the FEL system, which consists of two electromagnetic planar undulators, a magnetic buncher and an optical resonator. The FEL lasing at a wavelength of 0.12–0.23 mm and average power of 0.4 kW was extracted through the hole at the rear mirror. The FEL radiation was delivered to five user stations for the material and biological applications of the terahertz radiation [43].

The second stage of the accelerator-recuperator in a four-loop configuration is under construction. They plan to operate two FELs, one at the fourth orbit (40 MeV) and the other at the bypass of the second orbit (20 MeV). The recirculation loops are installed in the horizontal plane to share the linac and the injector with the single-loop terahertz FEL, which is installed in the vertical plane. Figure 17 shows a schematic representation of the second-stage accelerator-recuperator with four orbits in the horizontal plane and the first-stage terahertz FEL. The lasing of the 20-MeV FEL at the bypass of the

second orbit of the second-stage accelerator-recuperator was recently demonstrated with parameters: FEL wavelength of 40–80 μm , bunch charge of 1500 pC, bunch repetition of 7.5 MHz, and beam current of 9 mA [44].

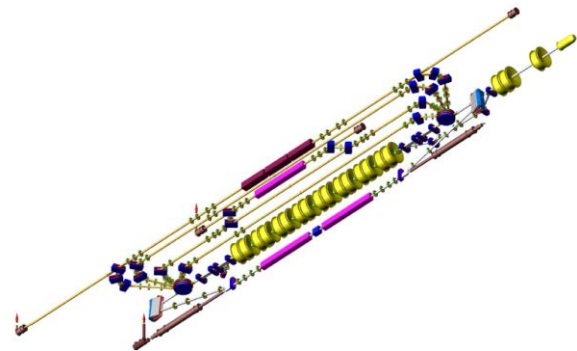


Figure 17. Schematic representation of the second stage of the accelerator-recuperator at BINP. Four orbits in the horizontal plane with two FELs are installed to share the main linac and the injector with the terahertz FEL in the vertical plane [44].

3.5. ALICE at Daresbury Laboratory

An ERL light source named 4GLS in the UK was proposed in 2001 as the provision of an advanced light source facility at lower energy to complement the DIAMOND X-ray light source [45, 46]. The 4GLS is a 600-MeV ERL used for delivering both CW beam currents up to 100 mA and alternatively high charge bunches for FEL applications. As an exploratory phase of the 4GLS, the construction of a smaller-scale ERL Prototype (ERLP) was funded in 2003 [47]. The ERLP was constructed inside the old building of the tandem accelerator at Daresbury Laboratory. The 4GLS project was unfortunately cancelled in early 2008 despite the intensive efforts of the community. Following the cancellation of the 4GLS, the ERLP facility changed its name to Accelerators and Lasers in Combined Experiments (ALICE) to serve as an advanced test

facility for novel accelerator and photon science applications [48].

Figure 18 shows the layout of ALICE. The electron gun is a copy of the 350-kV photo cathode DC gun at the JLAB IR-demo. The superconducting booster cavities for the injector and the main linac have an identical design: two 9-cell TESLA-like cavities in a cryomodule, which is based on the ELBE module. The injector cavities are operated at a low gradient, ~ 4 MV/m, to achieve the injection energy of 8.35 MeV. The main linac is operated at ~ 13 MV/m, and the final energy is 35 MeV. The return loop has two triple-bend achromatic arcs, a chicane-type bunch compressor, and an FEL wiggler.

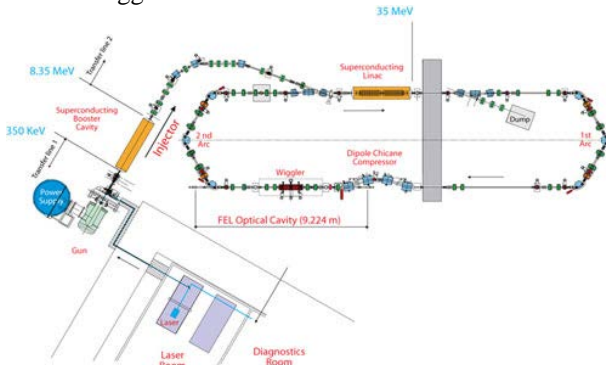


Figure 18. Schematic representation of ALICE at Daresbury Laboratory [47].

In the nominal operation mode, the high-voltage DC photoelectron gun is operated at a voltage of 350 kV

and a bunch charge of 80 pC. The bunch trains can be of variable length from a single bunch regime to 100 μ s with a bunch repetition frequency of 81.25 MHz within the train. The train repetition frequency can also be varied within the range of 1–20 Hz.

The first ERL operation was demonstrated on December 20, 2008. The energy recovery was confirmed by the rf power demand signals from the superconducting cavities of the main linac. In this experiment, the beam energy was 21 MeV, and the bunch charge was up to 20 pC [49]. The bunch charge and the beam energy were increased to be 40 pC and 27.5 MeV, respectively, in 2010 [50].

The facility ALICE is now operated as an experimental test-bed for a wide range of science and technology activities using an electron beam and ultra-short pulse lasers. For these activities, several light sources are under development: (1) an infrared FEL with a wavelength of ~ 4 μ m, (2) a THz source with coherent synchrotron radiation from sub-picosecond electron bunches passing through the final bending magnet of the chicane, and (3) a Compton back-scattered X-ray source with a photon energy of 15 or 30 keV. They already measured terahertz radiation, whose power showed quadratic dependence on the bunch charge, i.e., the indication of coherent emission.

The operation parameters of the demonstrated ERLs are summarized in Table 1.

Table 1. Operation parameters of the demonstrated ERLs *.

	1 st ERL operation	RF freq. (MHz)	RF pulse	Gun**	Bunch charge (PC)	Bunch rep. (MHz)	Beam current (mA)	Inj. Energy (MeV)	Loop energy (MeV)	Beam power (kW)	ref
IR-demo	1999	1498	CW	350 kV, PC	65	75	5	10	48	240	[19]
IR-upgrade	2003	1498	CW	350 kV, PC	135	75	9	10	160	1400	[17]
JAEA ERL	2002	499.8	1 ms, 10 Hz	230 kV, TC	450	20.8	9	2.5	17	150	[35]
BINP (1 st stage)	2003	180.4	CW	300 kV, TC	1500	22.5	30	1.8	11	330	[44]
BINP (2 nd stage)	2009	180.4	CW	300 kV, TC	1500	7.5	9	1.8	20	180	[44]
CEBAF	2003	1498	CW	100 kV, PC	0.16	499	0.08	55	1055	84	[37]
ALICE	2008	1300	0.1 ms, 1-20 Hz	230 kV, PC	40	81.25	3	3.9	27.5	89	[50]

* Some of parameters for BINP (2nd stage) and ALICE are tentative values during the commissioning.

** PC: photocathode, TC: thermionic cathode

4. Applications and Proposals of Future ERLs

Thus far, the ERLs have been developed and constructed for high-power FELs. The successful operation of such FELs has inspired applications of the ERL to a wider field of accelerator science and technology.

Accelerator-based light sources are the most promising application of ERLs. The emission of electromagnetic waves from relativistic electrons is possible in various ways, as listed in Table 1. Since the performance of these light sources is a function of electron beam parameters such as average current, emittance and pulse length, these light sources can be reinforced by ERLs producing electron beams of high average current, small emittance and short pulse length. The coherent synchrotron radiation from bunched electrons enables strong terahertz and millimeter waves. FELs can be operated in a wide range of photon energies from terahertz to X-rays. The synchrotron radiation from a bending magnet or an undulator is used for generating VUV, soft X-rays, and hard X-rays. Laser Compton scattering can generate X-ray and γ -ray beams.

Future light sources based on the ERL technology have been proposed across the world. We will discuss the proposals of X-ray and γ -ray light sources in the following sections.

Table 1. Possible ERL light sources in various regions of photon energy

Light source	Photon energy
Coherent synchrotron radiation	millimeter–terahertz
Free electron laser	millimeter–X-ray
Undulator radiation	VUV–X-ray
Laser Compton scattering	X-ray– γ -ray

4.1. X-ray Sources

An X-ray synchrotron light source is one of the most successful applications of high-energy electron accelerators. We can see across the world that more than 60 synchrotron light sources are now in operation to provide bright X-rays to many experimental uses from scientific researches to industrial applications. All the synchrotron light sources are based on storage rings.

The ERL with a high-average current and high-brightness electron beams can realize future synchrotron light sources, which outperform the storage-ring light sources in their X-ray spectral brightness and short-

pulse availability. The ERL X-ray light source was first proposed by a BINP group at the 1st Asian Particle Accelerator Conference in 1998; the proposed source was called “MARS – diffraction-limited 4th-generation X-ray source” [51].

The term “diffraction limit” refers to the condition in which an electron beam has smaller emittance than the emittance of the emitted photon beam. The photon beam has its intrinsic emittance determined by the uncertainty principle of the position and the momentum of the photons in the transverse plane. The intrinsic emittance of the photon beam in either the x or the y direction is given by $\varepsilon_{ph} = \lambda/(4\pi)$, where λ is the wavelength of the photon beam. Therefore, the condition for the diffraction limited electron beam is defined as

$$\varepsilon \leq \frac{\lambda}{4\pi},$$

where ε is the geometrical emittance of the electron beam. It is known that the geometrical emittance is reduced by the linear acceleration, which is the betatron oscillation damping of the transverse phase space. If we have an electron beam of normalized emittance $\varepsilon_n = 0.1$ mm-mrad at an injector and accelerate the beam to 6 GeV by a linac, the beam reaches the diffraction limit for hard X-rays of $\lambda = 0.1$ nm.

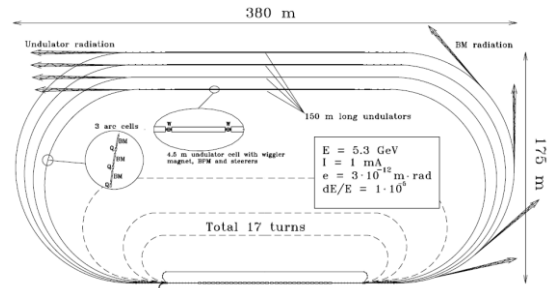


Figure 19. MARS–Multi-turn Accelerator Recuperator for a diffraction-limited 4th-generation X-ray light source [51].

The quality of an X-ray beam is characterized by, spectral brightness which is defined as the photon density in the six-dimensional volume:

$$B = \frac{F_{ph}}{4\pi^2 \sigma_x \sigma'_x \sigma_y \sigma'_y (d\omega/\omega)},$$

where F_{ph} is the photon flux, and σ_x , σ_y and σ'_x , σ'_y are the effective size and divergence of the photon source in

the x and y directions. The effective source size and divergence are the sum of the finite sizes and divergences of the electron and photon beams:

$$\begin{aligned}\sigma_x &= \sqrt{\sigma_{b,x}^2 + \sigma_{ph,x}^2}, \\ \sigma_y &= \sqrt{\sigma_{b,y}^2 + \sigma_{ph,y}^2}, \\ \sigma'_x &= \sqrt{\sigma_{b,x}^{\prime 2} + \sigma_{ph,x}^{\prime 2}}, \\ \sigma'_y &= \sqrt{\sigma_{b,y}^{\prime 2} + \sigma_{ph,y}^{\prime 2}},\end{aligned}$$

where subscripts b and ph refer to the electron beam and the photon beam, respectively. In the case of a negligible electron beam emittance, the spectral brightness becomes maximal and the photon beam is transversely coherent. For the diffraction-limited electron beam, the electron beam has the same size and divergence as the photon beam. In this case, the spectral brightness is 25% of the maximum value, and 25% of the photons are within the transversely coherent volume.

X-ray radiation from a diffraction-limited electron beam has superior coherence and is expected to promote a novel field of X-ray science such as coherent X-ray applications. The ERL X-ray source also promotes ultrafast X-ray science by utilizing sub-100fs electron bunches in the ERL, which can be generated by using the well-established technique of electron bunch compression.

In addition to the merit of small emittance for the high coherence, the ERL X-ray source has other advantages, which are a round beam, flexibility in electron beam optics and small energy spread [52].

The ERL X-ray source has near-isotropic transverse emittance, i.e. a round beam. An X-ray generated from the round beam has a coherent length same in the horizontal and vertical planes and can be easily transported and focused by X-ray optics such as a Fresnel zone plate. The ERL X-ray source with a round beam can also accommodate flexible undulators. The group of Cornell University developed the Delta undulator, which has a pure permanent magnet structure with 24 mm period and 5 mm diameter round gap. Using the Delta undulator, a 5-GeV ERL covers an X-ray energy range 3-12 keV with first harmonic radiation.

Storage ring X-ray sources are designed to have periodic or quasi periodic beam optics to keep electrons in a stable orbit for a number of turns. The ERL, in

contrast, allows flexible beam optics so that the horizontal and vertical betatron functions are tailored to insertion devices, either short or long undulator, for maximizing the spectral brightness.

Energy spread of electron beam in the ERL X-ray sources is dominated by curvature of rf acceleration field and expected to be 0.02% (rms) for a 2-ps bunch. This energy spread is smaller than that of storage rings, 0.1% (rms). The ERL, thus, can generate a narrow-band high-brightness X-ray from a long undulator with a large number of periods.

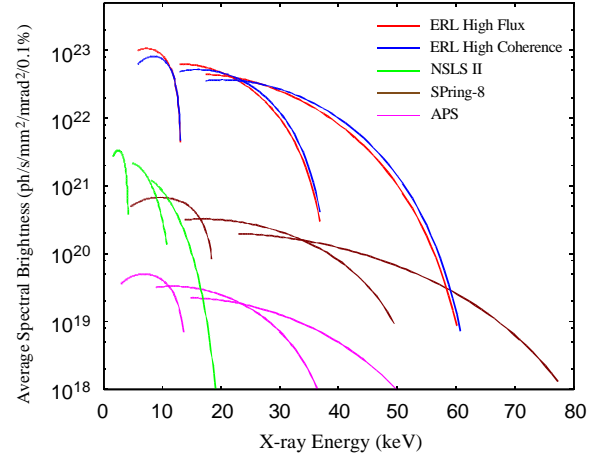


Figure 20. Average spectral brightness for a 5-GeV ERL and other storage ring X-ray sources.

In Fig. 20, we plot average spectral brightness for a 5-GeV ERL and storage rings. For the 5-GeV ERL, we assume parameters in Table 2 and a 25-m Delta undulator. Parameters for storage rings are retrieved from [52], SPring-8 (8 GeV, 25 m undulator), APS (7 GeV, 2.4 m undulator), NSLS-II (3 GeV, 3 m undulator). The spectral brightness was calculated by SPECTRA [53]. As seen in Fig. 20, the 5-GeV ERL has outstanding spectral brightness in a wide range of x-ray energy.

Research projects towards future ERL X-ray sources are carried out by Cornell University [54] and High Energy Acceleration Research Organization (KEK) [55]. In addition to these two facilities, an ERL upgrade program is under consideration at Advanced Photon Source at Argonne National Laboratory (ANL-APS) [56] and an ERL project is proposed at Helmholtz-Zentrum Berlin für Materialien und Energie GmbH (BESSY) [57].

Cornell University submitted a proposal in 2001 to build a 5-GeV ERL for an X-ray light source [54]. Figure 21 shows a layout of the Cornell 5-GeV ERL for the X-ray light source. In the ERL, an electron beam generated from a 10-MeV injector is accelerated by two superconducting linacs divided by a small turnaround arc. The existing Cornell Electron Storage Ring (CESR) tunnel is used for a return loop of the 5-GeV beam, and the undulator beam lines are installed in the beam transport paths before and after the CESR tunnel. The energy of each linac is designed to be asymmetrical, 2.3 GeV and 2.7 GeV, so that the accelerator and decelerator beams have separate orbits in the turnaround arc. During the operation of the ERL, the deceleration beam generally has a large emittance and a large energy spread in comparison with the acceleration beam. Therefore, transporting two beams independently in the turn around arc is helpful for the operation of the ERL at an optimum condition for preserving the small emittance during the acceleration and preventing the beam loss

Table 2. Operation modes of the Cornell 5-GeV ERL [58]

	High-flux	Coherence	Short pulse
Energy (GeV)	5	5	5
Current (mA)	100	25	0.1
Bunch charge (pC)	77	19	1000
Repetition rate (MHz)	1300	1300	0.1
Geometrical Emittance (μm)	30	8	500
Bunch length (ps)	2	2	<0.1
Relative energy spread	2E-4	2E-4	1E-3

They have developed an ERL injector targeting a normalized emittance of 0.1–1 mm-mrad and an average current of 100 mA, which fulfill the requirements of the 5-GeV ERL X-ray source. Some of their activities are described later.

A design study of an ERL light source was conducted in KEK, and a report was published in March

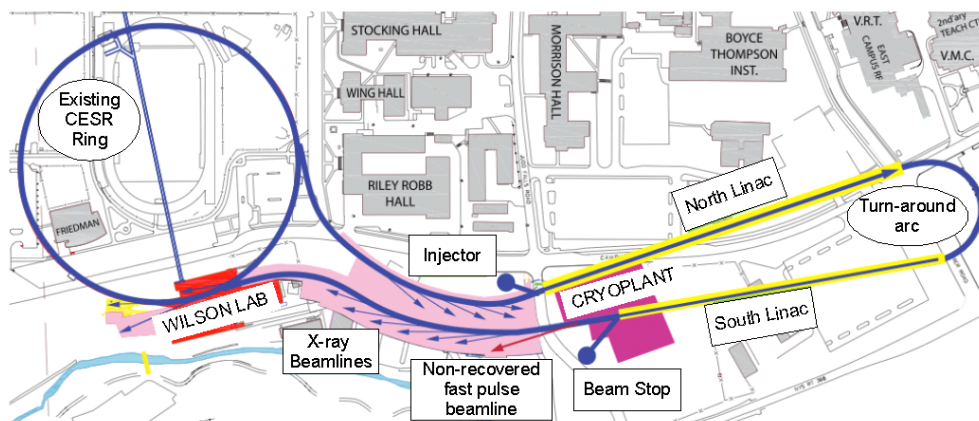


Figure 21. Schematic representation of the 5-GeV ERL for X-ray light source at Cornell University [58].

during the deceleration.

In the Cornell 5-GeV ERL, several operation modes are planned as listed in Table 2. The high-flux mode is used for obtaining high-flux X-rays from a beam of 100 mA, the maximum current. In the coherence mode, the diffraction-limited electron beam is utilized for generating X-rays with better coherence. The short-pulse mode is provided for the applications of sub-picosecond X-ray pulses. In the short-pulse mode, the electron beam goes to the beam dump before the deceleration, i. e., non-ERL operation because the small average current of 0.1 mA is available without energy recovery.

2003 [59], in which a 2.5–5 GeV ERL was proposed as a successor of the 2.5-GeV Photon Factory, a 2nd-generation light source in operation since 1985. The research group at JAEA, who developed the 17-MeV ERL-FEL, also designed a 6-GeV ERL light source independently of the KEK group [60]. Encouraged by the increasing global demands for the next-generation light sources, Japanese Society for Synchrotron Radiation Research (JSSRR) set up an ad-hoc committee to discuss next-generation light sources in Japan. The committee submitted, in 2006, a recommendation that an energy-recovery linac is the most promising candidate for an advanced ring-shaped

light source, which will lead them to the innovation of synchrotron radiation research in terms of both quality and quantity, and that national-wide research and development for future ERL light sources should be initiated immediately. Following this recommendation, KEK, JAEA and Institute of Solid State Physics, University of Tokyo (ISSP) negotiated for a possible collaboration on the development of ERL technologies and reached an agreement for the collaboration. The joint team involving members of KEK, JAEA, ISSP, SPring-8, and UVSOR started the R&D activities, including a high-brightness electron gun and superconducting cavities for the future ERL. They also decided to build a test facility of 35–245 MeV ERL as a prototype of their future ERL light sources [61, 62].

The 5-GeV ERL at the KEK site will be in a 2-loop system to accommodate the ERL within the 3-km circumference of KEK-B. The operation modes in the KEK ERL will be similar to those of the Cornell 5-GeV ERL.

4.2. Terahertz Sources

Coherent synchrotron radiation (CSR) is the emission of electromagnetic waves from electron bunches whose temporal duration is shorter than the radiation wavelength. The emitted power of CSR is proportional to N_e^2 , the square of the number of electrons in a bunch, while the power of incoherent synchrotron radiation (ISR) is proportional to N_e . Therefore, we can expect that the enhancement of the CSR power is 10^9 – 10^{10} for an electron bunch of 0.1–1 nC. CSR has been observed in electron linacs [63] and storage rings [64, 65], and applied to many experiments in the terahertz- and millimeter-wavelength region. The generation of high-power CSR from an ERL was demonstrated at the JLAB IR-demo [21]. Since an ERL can accelerate a high average current beam with short electron bunches, it can be a high-power CSR source to cover the terahertz region.

4.3. Laser Compton Scattering γ -ray Sources

A laser Compton scattering (LCS) γ -ray source is the only light source to produce γ -rays with good monochromaticity. The facilities of LCS γ -rays utilizing electron storage rings have been developed and used for nuclear and astrophysics applications [66, 67, 68, 69, 70]. Replacing the storage ring with the ERL, we can

improve the γ -ray monochromaticity and flux significantly.

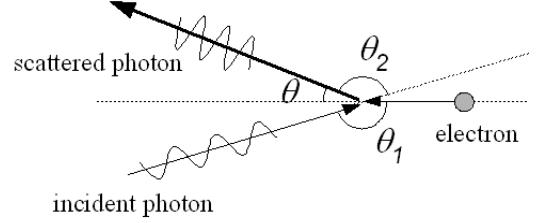


Figure 22. Schematic representation of laser Compton scattering.

Figure 22 shows a schematic representation of laser Compton scattering, where a high-energy photon (γ -ray) is generated via the Compton back-scattering of an incident laser photon with a relativistic electron. The energy of the scattered γ -ray photon, E_g , is a function of the incident photon energy, $E_L = hc/\lambda$, electron energy $E_e = \gamma mc^2$, and scattering geometry, and approximated for a head-on collision:

$$E_g \approx \frac{4\gamma^2 E_L}{1 + (\gamma\theta)^2 + 4\gamma E_L / (mc^2)}$$

The above equation shows that the γ -ray energy has a correlation to the scattered angle. Therefore, monochromatic γ -rays can be obtained by putting a collimator to restrict the γ -ray divergence downstream of the collision point.

However, the on-axis γ -ray through a collimator has a finite spectral broadening arising from the three-dimensional aspects of the interaction geometry and the energy spread of the laser and the electron beams. In the case of the head-on collision, the bandwidth of scattered γ -rays observed on the electron beam axis, $\theta = 0$, can be obtained by assuming the laser spot size w and the electron beam spot size σ as follows [71]:

$$\left(\frac{\Delta E_g}{E_g}\right)^2 = \left(\frac{\Delta E_L}{E_L}\right)^2 + \left(\frac{2\Delta\gamma}{\gamma}\right)^2 + \left(\frac{\lambda}{4\pi w}\right)^4 + \left(\frac{\varepsilon_n}{\sigma}\right)^4 \quad (1)$$

where the first term in the right-hand side is the spectral broadening due to the bandwidth of the incident laser pulse, the second term is the electron beam energy spread, the third term is the divergence of the laser beam, and the last term is the divergence of the electron beam. In LCS γ -ray sources utilizing storage rings, the on-axis

bandwidth is typically 2%–10%, which is restricted by the energy spread and the emittance of the electron beam.

In energy-recovery linacs, we can accelerate an electron beam of a smaller emittance and a smaller energy spread than those of the storage rings, for example the relative energy spread exhibited by CEBAF at high energy is under 2.5×10^{-5} [72]. As a result, LCS γ -rays from an ERL have an on-axis spectral width smaller than that of the LCS γ -rays from the storage rings. When the electron and the incident laser beams have the same spot size at the collision, $w = \sigma$, we can define the condition of a diffraction-limited electron beam from the last two terms in the right-hand side of Eqn. (1). The condition is that the γ -ray spectral broadening caused by the electron beam emittance becomes smaller than that caused by the laser photon emittance and given by

$$\varepsilon_n \leq \frac{\lambda}{4\pi}$$

The normalized emittance of the diffraction-limited electron beam is found to be 0.08 mm-mrad for an incident laser wavelength of 1 μm . This value of the normalized emittance is, accidentally, almost the same as the normalized emittance for the diffraction-limited hard X-ray light source for $\lambda=1 \text{ \AA}$. With the diffraction-limited electron beam from an ERL, the on-axis spectral width of the LCS γ -ray can be reduced to be 0.1% or less.

ERL-based LCS sources show outstanding performance when they are equipped with a laser supercavity for the colliding laser. The supercavity consists of mirrors with a high reflectivity. Optical pulses from an external mode-locked laser are stacked in the supercavity to attain a high average power. Supercavities having an enhancement factor of 10^3 – 10^4 are under development [73,74].

In the case of the Compton scattering, only a small fraction of electrons and photons contribute to the generation of high-energy photons because the cross section of the Compton scattering is very small. Therefore, the recycling of electrons and photons that do not contribute to the Compton scattering is necessary to realize a high-flux LCS source. The combination of an ERL and a laser supercavity is an ideal device for such recycling of electrons and photons.

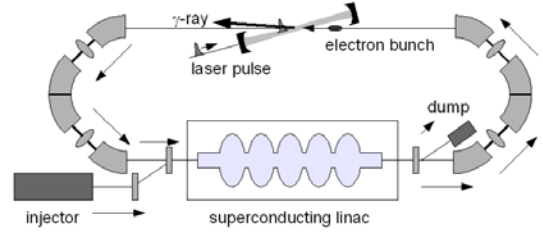


Figure 23. Schematic representation of LCS γ -ray source based on an ERL and laser supercavity [75].

Figure 23 is an LCS γ -ray source based on the combination of an ERL and a laser supercavity. The JAEA group conducted a design study of such γ -ray sources for nuclear industrial applications [75]. Using 350-MeV electron beams and 500–1000 nm lasers, we can generate γ -rays with energy up to 4.5 MeV. In their design, the γ -ray flux is expected to be 1×10^{13} ph/s in total, and spectral density 6.8×10^9 ph/s/keV for 2-MeV γ -rays, which exceeds the performance of the existing facilities based on the storage rings by 6–8 orders of magnitude. Such a high-flux energy-tunable γ -ray source with good monochromaticity can be used for many scientific and industrial applications. A nondestructive assay of radio-nuclides by using nuclear resonance fluorescence will be one of the promising applications.

5. Accelerator Technologies and Beam Dynamics Issues in Energy-Recovery Linacs

We have seen the ERL facilities ever built and the future applications of ERLs. In the design and construction of such ERLs, there are critical technologies of accelerator components and key issues of beam physics. Some of them have been resolved in the existing ERL facilities and some remains to be studied further. In this section, the beam dynamics issues in ERLs are reviewed briefly and development status of the two major components of ERLs, an electron gun and a superconducting cavity, is summarized. Detail studies on these subjects can be found in proceedings of past workshops [76]

5.1. Beam Dynamics Issues in ERLs

Generation of a small emittance beam from an injector

Since the emittance and current of an electron beam in an ERL are restricted by performance of its injector. Design of an injector for a small emittance and high-average current beam is one of the important tasks in the

development of ERLs. An ERL injector consists of an electron gun and injector superconducting cavities (SCA) to generate an electron beam at an energy of 5–10 MeV in a typical design. Additional components such as a buncher cavity, solenoid and quadrupole magnets are also installed along the injector. In the design of ERL injectors, emittance growth and its compensation should be considered in detail. The growth of emittance may occur due to space charge force and time-dependent rf focusing in the injector SCA.

A merger is a component specific to ERLs, which merges two beams—a low-energy injection beam and a high-energy recirculation beam—into the same trajectory. In storage rings, electron injection is usually made by a pulse kicker and a bump orbit. In ERLs, a combination of dipole magnets is used for the merger instead of a kicker, because the injection is conducted in the CW mode. Several designs of mergers are used in the ERLs: a three-dipole merger in the JLAB ERLs, a two-step staircase merger in the JAEA ERL, four-dipole chicane merger in the BINP ERL, and a zigzag merger in the ERL test facility in Brookhaven National Laboratory [77].

Generation and preservation of a small-emittance electron beam in an ERL injector and merger have been studied by multi-variant optimization technique, in which particle tracking simulations are carried out with scanning parameters of the buncher, solenoid, quadrupole and injector SCA to find a set of parameters for the smallest emittance [78,79].

Beam Instability due to Higher-Order Modes in Superconducting Cavities

Beam break up (BBU) induced by higher-order modes (HOMs) in superconducting cavities is a beam instability to restrict an electron beam current in a multi-pass recirculating accelerator [80]. In an accelerating cavity, a number of higher-order modes are excited by a bunched electron beam passing through the cavity. An HOM, which has a dipole field, may kick an electron bunch in a transverse direction. When the kicked electron bunch returns after the recirculation at a certain position and in a certain phase to excite the HOM, the HOM amplitude grows exponentially and the beam is finally lost because of the finite size of the beam aperture.

The HOM-BBU was an issue of concern in a superconducting microtron before the first ERL was constructed. In a 6-pass racetrack microtron at University of Illinois, MUSL-2, the HOM-BBU occurred at 0.3 μA , 67 MeV [81]. The superconducting cavity used in MUSL-2 was constructed by Stanford High-Energy Physics Laboratory. Since the cavity was designed to accelerate an electron beam having a small average current, it was equipped with neither HOM couplers nor an HOM absorber.

During the development of a CEBAF 5-pass recirculating linac, the HOM-BBU was studied in detail [82]. And the theory and simulations codes were further developed in the ERL projects. The BBU threshold current is defined as the beam current required to initiate the instability due to the HOM-BBU. The BBU threshold current for a simple geometry of a recirculating linac, a single cavity, a single HOM, and a single loop can be expressed in analytical formula [1,83]:

$$I_{th} = -\frac{2c^2}{e(R/Q)_\lambda Q_\lambda \omega_\lambda R_{12} \sin \omega_\lambda t_r},$$

where $(R/Q)_\lambda$, Q_λ , and ω_λ are the shunt impedance in the linac definition (in units of Ω), Q-value, and frequency of the HOM, respectively, R_{12} is the element of the recirculation transfer matrix, and t_r is the recirculation time. Therefore, a larger threshold current is obtained by using a smaller shunt impedance, smaller Q-value, and smaller R_{12} . The CEBAF cavity has waveguide-type HOM couplers to reduce the HOM Q values to the range of 10^4 – 10^5 . The BBU threshold current for the CEBAF 5-pass linac is calculated to be between 10 and 20 mA, which is two orders of magnitude above the maximum design current of 200 μA [84]. The JLAB IR-demo was constructed by using the CEBAF cavity and operated at a beam current of 5 mA without any indication of BBU.

In the JLAB IR-Upgrade, the HOM-BBU was observed at an average current of 3 mA, which is below the nominal 10-mA operation current for a 10-kW FEL [22]. The observation of BBU was precipitated by the installation of a new 7-cell cryomodule, in which several HOMs have loaded Q-values in the order of 10^6 corresponding to the BBU threshold current of 3–8 mA. In order to suppress the BBU in the IR-Upgrade, they adopted an optical suppression technique, in which betatron plane was rotated by 90° [85]. The rotation of

the betatron plane was achieved by the installation of five skewed quadrupole magnets in the return loop. As a result of the betatron phase rotation, electrons kicked by the dipole HOM with a horizontal polarization in a cavity at the first pass return to the cavity with an offset in the vertical direction at the second pass after the recirculation. Therefore, the electron at the second pass does not couple with the HOM with a horizontal polarization, and the HOM BBU is suppressed.

Specific design of superconducting cavity for suppression of the HOM-BBU is described later.

Beam Loss

Beam loss in an ERL must be kept as small as possible for maintaining the energy recovery and avoiding extra radiation. In a storage ring with a circumference of 1 km and a beam life of 10 h, the beam loss rate per single turn is calculated to be in the order of 10^{-11} . From this estimation of beam loss in a storage ring, we can conclude that beam loss in ERLs is a problem of radiation rather than energy recovery. Small but continuous beam loss in an ERL may cause serious problem in radiation safety and machine protection. Heat deposition in superconducting cavities due to beam loss results in local temperature rise and quenching of superconductivity. Beam loss is generated by beam halo, Touschek effect, scattering with residual gases, and so on.

Beam halo is produced by various processes. In a photo injector, illumination of a photocathode with stray light and amplified spontaneous emission from a drive laser generate beam halo. Dark current from a gun and superconducting cavities is another source of beam halo.

Touschek effect is a scatter of two electrons in a bunch via their mutual Coulomb force. Two electrons after the collision exchange some of their transverse momentum into the longitudinal direction, which may result in beam loss due to finite acceptance of dynamic or physical aperture. Beam loss of Touschek effect should be considered in ERLs, because electron beams of small emittance and short pulse length cause a high scattering rate. Studies on Touschek effect in ERL based X-ray light sources by particle simulations have shown that Touschek effect is serious in ERL-based X-ray light sources [86, 87]. Cautious management of beam loss by placement of collimators and appropriate sextupole corrections must be employed for minimizing radiation hazard.

Ion trapping is also a potential source of beam halo and particle loss in ERLs. Residual gases in a beam pipe are ionized during operation of ERLs by effects such as collisions and synchrotron radiation. The ions are trapped in a steep potential of electric field generated by electron beam of small transverse size. In order to avoid ion accumulations, a gap between electron bunches and clearing electrode were investigated [88].

In the JLAB IR Upgrade FEL, the beam loss at an operation of the ERL at 8 mA could be reduced in most of the accelerator to less than 100 nA and less than 10 nA in the wiggler. This small beam loss was achieved by matching the beam transport to the actual beam envelope including the halo [89]. Management of beam loss must be studied further in the ERL test facilities.

Preservation of emittance and energy spread

In addition to the above mentioned subjects, there are potential physics to increase beam emittance and energy spread in ERLs. Coherent synchrotron radiation (CSR) in a circular path introduces non-uniform energy change along the longitudinal position of electrons in a bunch. This energy change results in the growth of projection emittance after the circular path. Since the CSR effect has the larger impact for the shorter electron bunch, we must consider the CSR effect carefully in the design of ERLs for acceleration of short bunches, less than a few ps. For analysis of the CSR effects, numerical simulation codes are available and a beam transport design to compensate the CSR effect was proposed [90].

In an ERL with a long linac, emittance growth by coupler kicks, deflection of electrons by transverse field at the position of rf couplers, becomes a matter of concern. It has been shown that the coupler kicks can be compensated by methods: alternating the position and direction of the coupler each cavity; choosing the distance between coupler and cavity to minimize the coupler kick for on crest acceleration; and symmetrizing the coupler region by adding a stub opposite the coupler [91].

In the operation of ERLs, any relative energy spread introduced at high energy is amplified after the deceleration. Since the amplification factor is equal to the ratio between the high energy and the dump energy, management of the energy spread is indispensable in ERLs. As presented in Section 3.1, a technique of beam energy compression has been used in the JLAB high-power FEL [15]. Compensation of the wakefield-driven

energy spread was investigated in the configuration of 5-GeV ERL at Cornell, where time-of-flight terms in the ERL loop are used to reduce the wakefield-driven energy spread [92].

5.2. Electron Guns for ERLs

An electron gun used for producing small emittance electron beams with a high-average current is an essential device for an ERL to exploit its full advantages—the acceleration of high-power and high-brightness electron beams. For example, the proposed ERL X-ray sources are based on the following electron beam parameters: an average current of 10–100 mA, a normalized emittance of 0.1–1 mm-mrad, and a bunch repetition rate of 1.3 GHz. These parameters are beyond the established technologies of the existing electron guns.

Thus far, two types of electron guns have been utilized for the ERLs. One is a DC electron gun equipped with a gridded thermionic cathode, and the other is a DC electron gun with a photocathode. The former was adopted in JAEA ERL and BINP ERL. The latter was employed in JLab ERL and ALICE. In addition to the DC guns, superconducting rf gun and low-frequency normal conducting rf gun, are under development to produce small-emittance beams in a CW operation mode [93, 94]. In this section, we present an overview of the operation performance and the R&D status of the photocathode DC gun because this type of gun has the potential capability of producing diffraction limited electron beams in X-ray and γ -ray sources.

A photocathode DC gun can generate an electron beam having an ultra-small initial emittance when it is equipped with a semiconductor photocathode having a negative electron affinity (NEA) surface. Such an electron gun was first developed for polarized electron sources for nuclear physics applications. In CEBAF, 100-kV DC electron guns with an NEA cathode have been operated to provide an electron beam with a repetition rate of 499 MHz and maximum average current of 0.2 mA. A polarized electron beam is generated by using a drive laser pulse with circular polarization and a photocathode with a superlattice structure. In JLAB ERL FEL, a 350-kV DC gun has been operated at a beam current of 9 mA.

The advantages of this type of electron gun for ERL light source applications are a relatively large quantum efficiency and a small initial emittance. The electron beam current derived from a photocathode illuminated

by a laser pulse is a function of the quantum efficiency of the cathode, Q , the laser power, P , and the wavelength, λ :

$$I[\text{mA}] = \frac{1}{120} Q[\%] P[\text{W}] \lambda[\text{nm}]$$

A bulk GaAs photocathode has quantum efficiency (1%–10%) at a laser wavelength of 500–800 nm. An electron beam of 100 mA can be generated for parameters $Q = 2\%$, $P = 12 \text{ W}$, and $\lambda = 500 \text{ nm}$, which seem to be feasible by a combination of a bulk GaAs cathode and fiber laser technology.

In a photocathode DC gun, a high DC voltage is necessary for suppressing the emittance growth due to the space-charge force. From numerical simulations, it was found that a DC voltage higher than 500 kV is required for a future ERL X-ray light source [78]. For this purpose, many efforts have been devoted to the development of high-voltage DC guns.

Figure 24 shows a photocathode DC gun under development at JAEA. As seen in Fig. 23, the photocathode gun has a metallic rod to support a cathode electrode at the center of the gun vacuum chamber. This supporting rod limits the gun voltage. When a high voltage is applied to the gun, the field emission of the electrons from the supporting rod may occur. The electrons emitted from the supporting rod are intercepted by the inner surface of the ceramic and penetrate into the ceramic body. If the ceramic has a high resistivity, these electrons cause a concentration of charges in a small area and may lead to a punch-through failure of the ceramic.

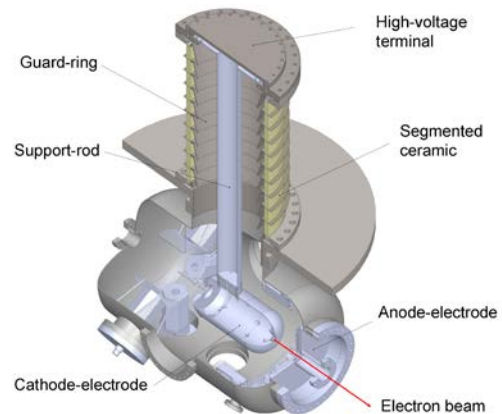


Figure 24. 500-kV photocathode DC gun at JAEA.

In Cornell University, ceramic insulators with a finite bulk resistivity and a finite surface resistivity have been tested to avoid such a failure [95].

In order to solve the field emission problem, a segmented ceramic insulator with guard rings was designed and fabricated in JAEA. This type of ceramic insulator is expected to be tolerant to the field-emitted electrons. The insulator consists of multiple ceramics stacked in series, and a Kovar electrode is sandwiched between two ceramics and blazed. Guard rings are attached to the Kovar electrode on both the inner and the outer sides. The amount of segmentation and the shape of the guard rings were optimized to minimize the surface electric field. The trajectories of field-emitted electrons from the rod were also taken into consideration in order to guard the ceramic surface from the field-emitted electrons from the supporting rod. A high-voltage test of the gun up to 550 kV was successfully achieved [96].

It is known that the tailoring of a three-dimensional distribution of an electron bunch generated from a photocathode can effectively reduce the space-charge emittance growth. Therefore, the shaping of a drive laser pulse has been an intrinsic technology in photocathode RF guns; this technology is also applicable to photocathode DC guns. In the scheme of the three-dimensional pulse shaping, the transverse direction is controlled by laser spatial shaping, and the longitudinal direction is achieved by laser temporal shaping. In the case of the temporal shaping, a photocathode must have a sufficient fast temporal response, typically less than a few picoseconds. In an experiment at Cornell University, it was revealed that such a fast temporal response can be obtained by an appropriate combination of the cathode material and the laser wavelength. In the experiment, a photocathode of GaAs illuminated by a 520-nm laser exhibited a temporal response that was faster than 2 ps [97], which is considerably faster than that for illumination with a near-band-gap wavelength (~800 nm). The faster response at 520 nm is attributed to the wavelength dependence of the optical absorption constant of GaAs.

For the practical operation of future ERL light source, a photocathode must provide an electron charge of more than 10000 C (100 mA, 1 day). The life of the NEA cathodes remains a critical issue to be resolved. The surface of a negative electron affinity is created by the coadsorption of Cs and O₂ (or NF₃) on a wafer of p-

doped GaAs. Since the NEA surface is easy to destroy by the collision of residual gas molecules or back-bombarding ions, the maintenance of a good vacuum is necessary to obtain long-life NEA cathodes. Therefore, DC photocathode guns are equipped with a vacuum chamber made of a material having a low out-gassing rate and a large capacity of NEG pumps.

In the Cornell DC gun, stainless steel that is heat-treated in air at 400°C is used for the vacuum chambers to obtain an out-gassing rate of 3×10^{-11} Pa m/s [98]. The main chamber is equipped with NEG pumps, 20000 L/s in total.

In JAEA, they fabricated vacuum chambers made of titanium having an out-gassing rate of 6×10^{-13} Pa m/s. The main chamber of the JAEA DC gun accommodates 18000 L/s NEG pumps and a 500-L/s ion pump [99].

The off-center illumination of a drive laser is also effective in obtaining a relatively long life of the NEA cathodes. This is because the back-bombarding ions hit the center of the photocathode, a position different from the electron emission area. In the JLAB FEL gun with off-center illumination, they obtained a cathode lifetime (1/e life) of 550 C at 5-mA operation [100].

The optimization of the electrode geometry to preserve a small beam emittance during the off-center illumination is yet to be studied.

5.3. Superconducting Cavities for ERLs

The superconducting accelerator (SCA) for a high-average current electron beam is another critical component in the ERL. The research items of SCA include a high-power input coupler, an efficient damping of higher-order modes (HOM), cryomodules with small microphonics, a low-level rf controller for the precise control of rf amplitude and phase, and a superconducting cavity itself.

The superconducting cavity for the ERL is divided into two categories, one for an injector and the other for a main linac. In the injector cavity, an electron beam having a high-average current is accelerated without energy recovery, i.e., powered by external rf sources. Therefore, a high-power input coupler is a critical component to be developed. In Cornell University, an L-band 2-cell cavity was developed for an ERL injector [101]. The cavity is equipped with two couplers, each of which feeds 50-kW rf power into the cavity. The couplers are installed as they face each other to cancel a dipole kick of couplers and preserve the beam emittance.

Ceramic tiles for the HOM absorbers are installed along the inner surface of the beam pipe at both ends of the cavity. Figure 25 shows a photograph of the Cornell 2-cell cavities. They constructed an ERL injector test facility, which consists of a photocathode DC gun and an injector cryomodule to contain five 2-cell cavities [102]. The injector is designed to produce an electron beam having a 500-kW power. The commissioning of the injector is in progress.

An injector cavity developed by KEK also has an L-band 2-cell shape, as shown in Fig. 26 [103]. The cavity has twin couplers similar to Cornell's cavity, but the KEK coupler can support a higher rf power, 150 kW per coupler. The high coupler power is attributed to the use of a coaxial ceramic window, TRISTAN type window, instead of the cylindrical window used in the Cornell and TESLA couplers. The coaxial window for the KEK ERL cavity is similar to STF-baseline coupler developed by KEK for International Linear Collider R&D. The KEK group is developing an injector cryomodule, which contains three 2-cell cavities, to accelerate a 1-MW beam. The cavity has five HOM couplers for damping HOMs.



Figure 25. Injector cavity developed at Cornell University. The cavity has a 2-cell shape and is operated at 1.3 GHz [58].



Figure 26. Injector cavity developed at KEK. The cavity has a 2-cell shape and is operated at 1.3 GHz. Five HOM couplers are installed at both sides of the beam pipe [103].

In the design of 100-mA class ERLs for future light sources, HOM BBU should be suppressed by a combination of the following techniques: (1) the use of superconducting cavities with small Q-values of HOMs, (2) the randomization of HOM frequencies over many cavities, and (3) the optimization of recirculation beam optics. Here, we summarize research activities on superconducting cavities for the acceleration of high-average current beams in future ERL light sources.

The Japanese collaboration team (KEK / JAEA / ISSP) is developing superconducting cavities for future ERL light sources. They have chosen a 9-cell 1.3-GHz structure and obtained a cavity design to achieve an HOM-BBU threshold current of more than 600 mA in a 5-GeV ERL. The cavity has an optimized cell shape, enlarged beam pipes for efficient damping of HOMs, and eccentric-fluted beam pipe for damping the quadrupole HOMs. HOMs excited in the cavity are extracted through the beam pipes and damped by on-axis HOM absorbers installed at both ends of the cavity [104].



Figure 27. ERL cavity developed by KEK/JAEA/U-Tokyo. The cavity has a 9-cell shape and is operated at 1.3 GHz [104].

A superconducting cavity for an ERL main linac is also under development at Cornell University. The cavity has a 7-cell shape and is operated at 1.3 GHz [105]. The cavity shape was optimized to accomplish a small dynamic heat load of the accelerating mode, maintain a low ratio of the peak electric to accelerating field to minimize the risk of the field emission, reduce the Q-values of the HOMs for a large threshold current of HOM-BBU and increase cell-to-cell coupling for reduced occurrence of trapped modes with production errors. The BBU threshold current of the cavity is estimated to be $>250\text{mA}$ for the 5-GeV ERL under proposal at Cornell University. A cryomodule to accommodate two 7-cell cavities is under fabrication by the international collaboration of Cornell and Stanford Universities, Daresbury Laboratory, DESY, FZD-Rossendorf, Lawrence Berkley Laboratory, and TRIUMPH. The cryomodule will be installed in the

ALICE ERL accelerator at Daresbury Laboratory and validated with an electron beam in 2010 [106].

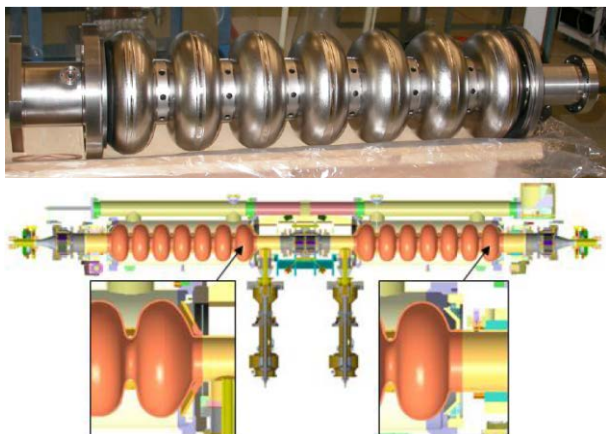


Figure 27. ERL cavity developed by Cornell University and ERL cavity string assembly for the international cryomodule testing. The cavity has a 7-cell shape and is operated at 1.3 GHz [105, 106].

6. Other ERLs

The principle of energy recovery is very simple: the reinjection of a spent electron beam into an rf linear accelerator at a deceleration phase. The energy conversion from the spent beam to the rf is guaranteed by electromagnetic theory. This simplicity makes the ERL a universal technology applicable to various fields. In addition to the light source applications discussed here, several proposals of ERLs have been submitted. In Brookhaven National Laboratory, they plan to utilize an ERL for the electron cooling of hadron beams in RHIC-II, the near-term upgrade of Relativistic Heavy Ion Collider (RHIC) [107]. Moreover, two types of electron-ion colliders based on the ERL technology are proposed for a future plan of RHIC: eRHIC (high-energy electron-ion collider) [108] and MeRHIC (medium-energy electron-ion collider) [109]. An ERL-based lepton-hadron collider (LHeC) is also proposed at CERN as a future upgrade of LHC [110].

7. Summary and Outlook

We have reviewed the energy-recovery linac for light source applications, tracing the history of ERLs over 40 years. The ERL was initially proposed for an electron collider and later developed for high-power FELs. The ERL is currently considered an important platform of future light sources covering a wide range of photon energy from terahertz to X and γ -rays.

Among the possible light source applications utilizing ERLs, the X-ray synchrotron facilities to produce coherent X-rays and ultrashort X-rays play a leading role to promote the R&D of the accelerator components specific to the ERLs. Two major components of the ERL, CW electron gun and superconducting cavity, are under intense development for the future ERL light sources. The complete performance of such components to obtain an electron beam of 10–100 mA with an emittance of 0.1–1 mm-rad has not been demonstrated yet. However, the critical research items towards the target performance have been resolved one by one.

The test facilities to prove the performance of such components are in operation and under construction. The injector test facility at Cornell University was constructed to demonstrate the complete performance of the “ERL quality” beam, 10–100 mA and 0.1–1 mm-rad. All the injector components, a photocathode DC gun, a buncher, an injector superconducting module, high-power klystrons, and a merger, have been developed. The beam performance is currently limited by a gun voltage of 250 kV, which is lower than the design value, 500–750 kV. They continue to improve the gun voltage by modifying a ceramic insulator. Another test facility, the Compact ERL at KEK, will be completed in 2012. The facility is a small-size ERL with an injector, main linac, and recirculation loop. The Compact ERL is designed to accommodate an electron beam of 245 MeV and 100 mA, but will be operated in a smaller beam power in the initial stage, 35 MeV and 10 mA. We are convinced that the “ERL quality” beam will be demonstrated in these facilities in the near future.

References

1. L. Merminga, D.R. Douglas and G.A. Krafft, *Annu. Rev. Nucl. Part. Sci.* **53**, 387 (2003).
2. M. Tigner, *Nuovo Cimento* **37**, 1228 (1965).
3. S. O. Schriber et al., *IEEE Trans. on Nucl. Sci.*, **NS-24**, 1061 (1977).
4. J. M. J. Maday, *J. Appl. Phys.* **42**, 1906 (1971).
5. L. R. Elias et al., *Phys. Rev. Lett.* **36**, 717 (1976).
6. D. A. G. Deacon, et al., *Phys. Rev. Lett.* **38**, 892 (1977).
7. C. A. Brau et al., US Patent 4,323,875, Apr. 6, 1982.
8. L. R. Elias, *Phys. Rev. Lett.* **42**, 977 (1979).
9. L. R. Elias, J. Hu and G. Ramian, *Nucl. Instr. Meth.* **A237**, 203 (1985).

10. D. W. Feldman et al., *Nucl. Instr. Meth.* **A259**, 26 (1987).
11. T. I. Smith et al., *Nucl. Instr. Meth.* **A259**, 1 (1987).
12. G. R. Neil, Proc. PAC-1995, 137 (1996)
13. F. H. Dylla et al., Proc. PAC-1995, 102 (1996).
14. J. B. Flanz and C. P. Sargent, *Nucl. Instr. Meth.* **A241**, 325 (1985).
15. P. Piot, D. R. Douglas and G. A. Krafft, *Phys. Rev. ST-AB* **6**, 030702 (2003).
16. G. R. Neil et al., *Phys. Rev. Lett.* **84**, 662 (2000).
17. G. R. Neil et al., *Nucl. Instr. Meth.* **A557**, 9 (2006).
18. D. Douglas, S. V. Benson, G. A. Krafft, R. Li, L. Meringa and B. C. Yu, Proc. LINAC-2000, 857 (2000).
19. S. V. Benson, *Nucl. Instr. Meth.* **A483**, 1 (2002).
20. C. Behre et al., *Nucl. Instr. Meth.* **A528**, 19 (2004).
21. G. L. Carr et al., *Nature* **420**, 153 (2002).
22. C. D. Tennant et al., *Phys. Rev. ST-AB* **8**, 074403 (2005).
23. Y. Kawarasaki, M. Ohkubo, N. Shikazono and K. Mashiko, *Nucl. Instr. Meth.* **A272**, 206 (1988).
24. Y. Kawarasaki et al., *Nucl. Instr. Meth.* **A285**, 338 (1989).
25. M. Takao et al., *Nucl. Instr. Meth.* **A331**, 218 (1993).
26. M. Takao et al., *Nucl. Instr. Meth.* **A341**, 394 (1994).
27. E. Minehara et al., *Nucl. Instr. Meth.* **A429**, 9 (1999).
28. N. Nishimori et al., *Nucl. Instr. Meth.* **A445**, 432 (2000).
29. N. Nishimori, R. Hajima, R. Nagai and E. J. Minehara, *Nucl. Instr. Meth.* **A475**, 266 (2001).
30. E. J. Minehara, *Nucl. Instr. Meth.* **A483**, 8 (2002).
31. N. Nishimori, R. Hajima, R. Nagai and E. J. Minehara, *Phys. Rev. Lett.* **86**, 5707. (2001).
32. R. Hajima et al., *Nucl. Instr. Meth.* **A445**, 384 (2000).
33. R. Hajima and E. J. Minehara, *Nucl. Instr. Meth.* **A507**, 141 (2003).
34. R. Hajima et al., *Nucl. Instr. Meth.* **A507**, 115 (2003).
35. N. Nishimori et al., Proc. FEL-2006, 265 (2006).
36. R. Hajima et al., Proc. FEL-2005, 301, (2005).
37. A. P. Freyberger et al., Proc. EPAC-2004, 524 (2004).
38. H. A. Grunder et al., Proc. PAC-1987, 13 (1987).
39. C. W. Leeman, D. R. Douglas and G. A. Krafft, *Annu. Rev. Nucl. Part. Sci.* **51**, 413 (2001).
40. N. G. Gavrilov et al., *Nucl. Instr. Meth.* **A304**, 228 (1991).
41. V. S. Arbuzov et al., Proc. RuPAC-2004, 318 (2004).
42. E. A. Antokhin et al., *Nucl. Instr. Meth.* **A528**, 15 (2004).
43. N. G. Gavrilov et al., *Nucl. Instr. Meth.* **A575**, 54 (2007).
44. N. A. Vinokurov et al., Proc. IPAC-2010, WEOARA03 (2010)..
45. J. A. Clarke et al., Proc. PAC-2001, 253 (2001).
46. M. W. Poole et al., Proc. PAC-2003, 189 (2003).
47. M. W. Poole and E. A. Seddon, Proc. EPAC-2004, 455 (2004).
48. D. J. Holder, Proc. LINAC-08, 694 (2008).
49. J. Alexander et al., Proc. PAC-09, TU5RFP083 (2009)
50. Y. Saveliev et al., Proc. IPAC-2010, TUPE096 (2010).
51. D. A. Kayran et al., Proc. APAC-1998, 6D015 (1998).
52. D. H. Bilderback et al., *New J. Phys.* **12**, 035011 (2010).
53. SPECTRA version 8.0.8, <http://radiant.harima.riken.go.jp/spectra/>
54. Sol M. Gruner et al., *Rev. Sci. Instr.* **73**, 1402 (2002).
55. T. Kasuga et al., Proc. APAC-07, TUPMA046.
56. M. Borland, G. Decker, A. Nassiri, Y. Sun, and M. White, Proc. of AccApp'07, pp. 196-203 (2007).
57. W. Anders et al., Proc. SRF-2009, 223 (2009).
58. G. Hoffstaetter, Proc. Future Light Workshop 2010 (2010).
59. "Study Report on the Future Light Source at the Photon Factory –Energy Recovery Linac and Science Case–", T. Suwada and A. Iida ed. (2003) (in Japanese).
60. R. Nagai et al., Proc. PAC-03, 3443 (2003).
61. "Design Study of the Compact ERL", R. Hajima, N. Nakamura, S. Sakanaka, Y. Kobayashi ed., KEK Report 2007-7 / JAEA-Research 1008-032 (2008) (in Japanese).
62. S. Sakanaka et al., Proc. IPAC-2010, TUPE091 (2010).
63. T. Nakazato et al., *Phys. Rev. Lett.* **63**, 1245 (1989).
64. M. Abo-Bakr et al., *Phys. Rev. Lett.* **90**, 094801 (2003).
65. Y. Takashima et al., *Jpn. J. Appl. Phys.* **44**, L1131 (2005).
66. V. N. Litvinenko et al., *Phys. Rev. Lett.* **78**, 4569 (1997).
67. H. R. Weller et al., *Prog. in Part. and Nucl. Phys.* **62**, 257 (2009)
68. H. Ohgaki, H. Toyokawa, K. Kudo, N. Takeda and T. Yamazaki, *Nucl. Instr. Meth.* **A455**, 54 (2000).
69. K. Aoki et al., *Nucl. Instr. Meth.* **A516**, 228 (2004).

70. V. Nelyubin, M. Fujiwara, T. Nakano and B. Wojtsekhowski, *Nucl. Instr. Meth.* **A425**, 65 (1999).
71. W. J. Brown and F. V. Hartemann, *Phys. Rev. ST-AB* **7**, 060703 (2004).
72. G. A. Krafft et al., *Proc. XX Int. Linear Acc. Conf.*, 721 (2000).
73. K. Sakaue et al., *Proc. EPAC-08*, 1872 (2008).
74. V. Brisson et al., *Nucl. Instr. Meth.* **A608**, S75 (2009).
75. R. Hajima et al., *J. Nucl. Sci. Technol.* **45**, 441 (2008).
76. Proc. ERL Workshops in 2005, 2007 and 2009; Proc. Future Light Source Workshops in 2006 and 2010. <http://www.jacow.org/>
77. V. N. Litvinenko, R. Hajima, D. Kayran, *Nucl. Instr. Meth.* **A557**, 165 (2006).
78. I. V. Bazarov, *Phys. Rev. ST-AB* **8**, 034202 (2005).
79. R. Hajima and R. Nagai, *Nucl. Instr. Meth.* **A557**, 103 (2006).
80. E. Pozdeyev, C. Tennant, J.J. Bisognano, M. Sawamura, R. Hajima and T.I. Smith, *Nucl. Instr. Meth.* **A557**, 176 (2006).
81. P. Axel et al., *Proc. PAC-1979*, 3143 (1979).
82. G. A. Krafft and J. J. Bisognano, *Proc. PAC-87*, 1356 (1987).
83. G.H. Hoffstaetter and I.V. Bazarov, *Phys. Rev. ST Accel. Beams* **7**, 054401 (2004)
84. N.S. Sereno and L.S. Cardman, *Proc. PAC-1993*, 3246 (1993).
85. R. E. Rand and T. I. Smith, *Part. Accel.* **11**, 1 (1980).
86. G. H. Hoffstaetter et al, *Proc. EPAC-08*, 1631 (2008).
87. A. Xiao and M. Borland, *Phys. Rev. ST Accel. Beams* **13**, 074201 (2010).
88. G. H. Hoffstaetter and M. Liepe, *Nucl. Instr. Meth.* **A557**, 205 (2006).
89. S. Benson et al., *Proc. PAC-07*, 79 (2007).
90. G. Bassi et al., *Nucl. Instr. Meth.* **A557**, 189 (2006).
91. B. Buckley and G. H. Hoffstaetter, *Phys. Rev. ST Accel. Beams* **10**, 111002 (2007).
92. G. H. Hoffstaetter and Y-H. Lau, *Phys. Rev. ST Accel. Beams* **11**, 070701 (2008).
93. A. Arnold et al., *Nucl. Instr. Meth.* **A577**, 440 (2007).
94. J. Baptiste et al., *Nucl. Instr. Meth.* **A599**, 9 (2009).
95. C. K. Sinclair, *Nucl. Instr. Meth.* **A557**, 69 (2006).
96. R. Nagai et al., *Rev. Sci. Instr.* **81**, 033304 (2010).
97. I. V. Bazarov et al., *Phys. Rev. ST-AB* **11**, 040702 (2008).
98. C. D. Park et al., *J. Vac. Sci. Technol.* **A26**, 1166 (2008).
99. R. Hajima et al., *Proc. PAC-09*, MO6RFP074 (2009).
100. C. Hernandez-Garcia, *AIP Conf. Proc.* **1149**, 1071 (2009).
101. V. Shemelin, S. Belomestnykh, R. L. Geng, M. Liepe, H. Padamsee, *Proc. PAC-03*, 2059 (2003).
102. M. Liepe et al., *Proc. SRF-2009*, 27 (2009).
103. S. Noguchi, E. Kako, M. Satoh, T. Shishido, K. Watanabe and Y. Yamamoto, *Proc. IPAC-2010*, WEPEC024 (2010).
104. K. Umemori, T. Furuya, H. Sakai, T. Takahashi, K. Shinoue and M. Sawamura, *Proc. SRF-2009*, 355 (2009).
105. N. Valles and M. Liepe, *Proc. SRF-2009*, 538 (2009).
106. P.A. McIntosh et al., *Proc. SRF-2009*, 864 (2009).
107. I. Ben-Zvi, *Proc. SRF-2007*, 740 (2007).
108. V. Ptitsyn et al., *Proc. of Hadron Beam 2008*, WGE01 (2008).
109. Y. Hao et al., *Proc. IPAC-2010*, TUPEB042 (2010).
110. F. Zimmermann et al., *Proc. IPAC-2010*, TUPEB039 (2010).